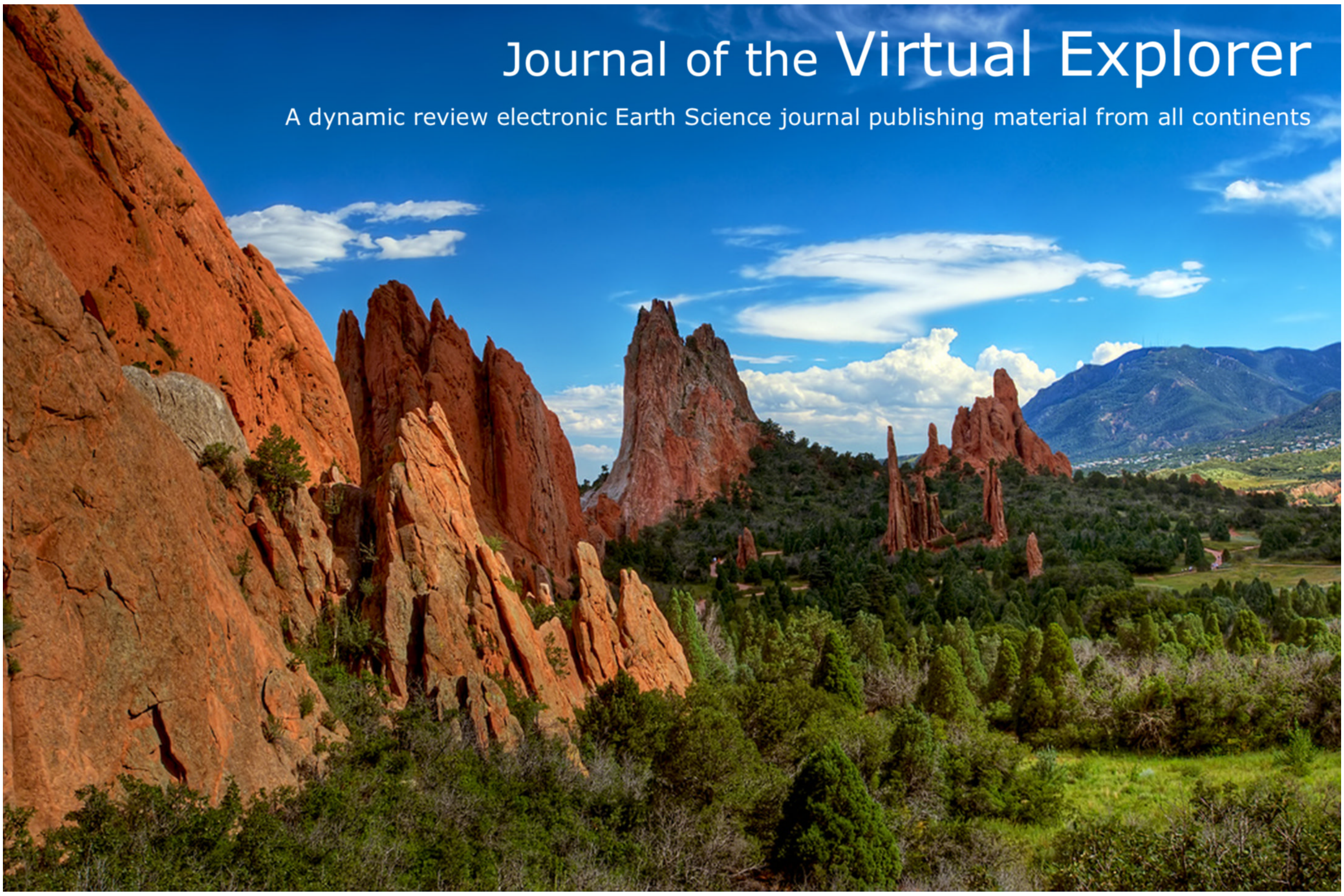

Visualisation of active normal fault scarps in the Apennines, Italy: a key to assessment of tectonic strain release and earthquake rupture.

Gerald P. Roberts

Journal of the Virtual Explorer, Electronic Edition, ISSN 1441-8142, volume **29**, paper 4
In: (Ed.) Declan De Paor, Google Earth Science, 2008.

Visualisation of active normal fault scarps in the Apennines, Italy: a key to assessment of tectonic strain release and earthquake rupture.

Gerald P. Roberts

Journal of the Virtual Explorer, Electronic Edition, ISSN 1441-8142, volume **29**, paper 4
In: (Ed.) Declan De Paor, Google Earth Science, 2008.

Abstract: Active normal fault scarps that offset 12-18 ka landforms in the Apennines, Italy, have been mapped into Google Earth to provide precise locations for structures responsible for tectonic strain release and earthquake rupture. Climate change at the end of the last glacial maximum (12-18 ka) reduced erosion and sedimentation rates below a critical threshold allowing preservation of displacements produced by surface ruptures to palaeoearthquakes. The resultant fault scarps, which record the surface displacements from multiple earthquakes, allow determination of the spatial variation in the rates of fault slip, a parameter critical to assessment of how long-term strain release recorded in the geomorphology (10^4 years) relates to short-term strain release recorded by earthquake catalogues and geodesy (10^{2-3} years). Spatial variation in fault slip occurs at a scale of tens of kilometres, whilst fault scarps have offsets of <20-40 metres and a geomorphic expression that can only be visualised on topographic images with spatial resolution approaching the metre-scale. Thus, until now, debate has surrounded the exact positions of scarps at least in part due to problems of visualising both the detailed geomorphic features and their regional variation. Provision of complete SPOT image coverage and topography within Google Earth allows individual scarps visited during fieldwork to be visualised at a regional scale within an easily-accessible interface. The resultant maps are used to comment on tectonic strain release and earthquake rupture.

http://virtualexplorer.com.au/article/2008/197/active-normal-fault-scarps-in-the-apennines

Citation: Roberts, G. 2008. Visualisation of active normal fault scarps in the Apennines, Italy: a key to assessment of tectonic strain release and earthquake rupture.. In: (Ed.) Declan De Paor, *Journal of the Virtual Explorer*, volume **29**, paper 4, doi: 10.3809/jvirtex.2008.00197

Introduction

The Italian Apennines suffers devastating earthquakes related to the ongoing crustal extension in this part of the convergent boundary between the African and European tectonic plates (e.g. 1915 Fucino Earthquake Ms 6.9, 33,000 deaths; Margottini and Screpanti 1988, Anderson and Jackson 1987) (Figure 1a).

Figure 1. Active faults of the Italian Apennines

Figure 1. Map of active faults for the Italian Apennines. Active faults are defined by clear structural offsets that have formed since 12-18 ka. These offsets are evidenced by limestone bedrock fault scarps offsetting landforms from 12-18 ka that can be seen clearly on Google Earth. Such offsets are accompanied by landforms that can be seen on Google Earth such as incised of footwall drainage, triangular facets, and oversteepened bases to footwall fault escarpments. See the accompanying "kmz" file to zoom into this view and visualise the landforms. Red lines show faults visited in the field. White lines show faults not visited in the field but with relatively clear geomorphic expression as seen on Google Earth. Figure 6 shows an interpretation of the lateral continuity of active faults, where the view in this figure has been combined with structural measurements such as total throw, throw since 12-18 ka, and kinematic data revealing the slip-directions associated with the extensional tectonics. More active faults exist to tthe northwest and southeast of the area considered in this paper. Boxes locate Figures 2, 3 and 4. Precise geographic coordinates for the fault scarps can extracted from the "paths" in the "kmz" file (e.g. Fig. 5).

Map of active faults for the Italian Apennines. Active faults are defined by clear structural offsets that have formed since 12-18 ka. These offsets are evidenced by limestone bedrock fault scarps offsetting landforms from 12-18 ka that can be seen clearly on Google Earth. Such offsets are accompanied by landforms that can be seen on Google Earth such as incised of footwall drainage, triangular facets, and oversteepened bases to footwall fault escarpments. See the accompanying "kmz" file to zoom into this view and visualise the landforms. Red lines show faults visited in the field. White lines show faults not visited in the field but with relatively clear geomorphic expression as seen on Google Earth. Figure 6 shows an interpretation of the lateral continuity of active faults, where the view in this figure has been combined with structural measurements such as total throw, throw since 12-18 ka, and kinematic data revealing the slip-directions associated with the extensional tectonics. More active faults exist to tthe northwest and southeast of the area considered in this paper. Boxes locate Figures 2, 3 and 4. Precise geographic coordinates for the fault scarps can extracted from the "paths" in the "kmz" file (e.g. Fig. 5).

Such earthquakes produce surface ruptures that are 15-20 km in length and have surface offsets of about 1 metre along pre-existing faults (Serva et al. 1986, Wells and Coppersmith 1994). The historical earthquake catalogue for the Apennines records events that have damaged Rome back to Roman times, and the catalogue is thought to be complete for large magnitude events (>Ms 6.0) since 1349 A.D.. However, the recurrence times for such large earthquake are 500-3000 years, recorded through palaeoseismological trench investigations (e.g. Michetti et al. 1996, Pantosti et al. 1996), so a longer record of fault slip is needed to assess the relationship between long-term strain release recorded in the geomorphology (10^4 years) and short-term strain release recorded by earthquake catalogues and geodesy (10^{2-3} years). A key observation is that the cumulative effect of such earthquakes over 10^4 year timescale has been preserved due to the fact that the rate of vertical offset of the ground surface across faults (0.2-2.0 mm/yr; Roberts and Michetti 2004, Papanikoloau and Roberts 2007) is higher than erosion and sedimentation rates since the last glacial maximum (12-18 ka) (Figure 1b). The timing of surface offsets for this 12-18 ka timescale have been constrained by palaeoseismological trench investigations (Michetti et al. 1996, Pantosti et al. 1996), tephrachronology (e.g. Giraudi 1995), and ^{36}Cl cosmogenic surface exposure dating of fault planes that emerge out of the ground along the scarps during earthquakes (Palumbo et al. 2006) (Figure 2a) and (Figure 2b).

Figure 2a. Fault scarps on SPOT images

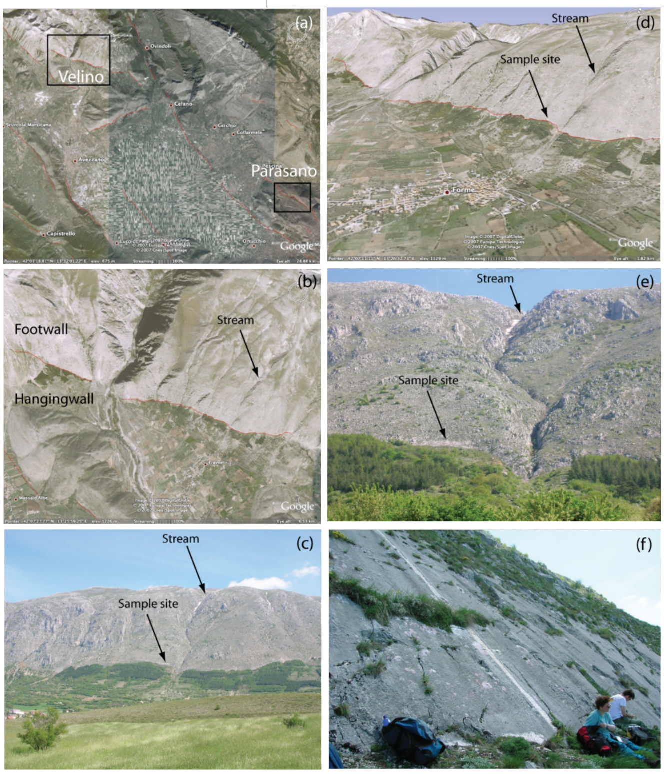

Figure 2. Examples of fault scarps visible at outcrop and on SPOT images (a) Overview locating the Velino and Parasano fault scarps. (b) Google Earth view of the Velino fault scarp. The fault separates Mesozoic limestones from Quaternary colluvium, and this is responsible for the vegetation change at the scarp. Note that incised drainage and triangular facets terminate at the fault scarp. (c) Outcrop photo showing the incised footwall drainage and ^{36}Cl sample site on the Velino Scarp. (d) Google Earth 3D view of the Velino Scarp. (e) Detail of the Velino fault scarp showing the ^{36}Cl sampling site from Palumbo et al. (2006). (f) View of the fault plane exposed along the fault scarp. The white line is ^{36}Cl sample site. Continued on next page.

Examples of fault scarps visible at outcrop and on SPOT images (a) Overview locating the Velino and Parasano fault scarps. (b) Google Earth view of the Velino fault scarp. The fault separates Mesozoic limestones from Quaternary colluvium, and this is responsible for the vegetation change at the scarp. Note that incised drainage and triangular facets terminate at the fault scarp. (c) Outcrop photo showing the incised footwall drainage and ^{36}Cl sample site on the Velino Scarp. (d) Google Earth 3D view of the Velino Scarp. (e) Detail of the Velino fault scarp showing the ^{36}Cl sampling site from Palumbo et al. (2006). (f) View of the fault plane exposed along the fault scarp. The white line is ^{36}Cl sample site.

Figure 2b. Fault scarps on SPOT images (cont.)

Figure 2 continued. (g) Overview of the Parasano Scarp. (h) Interpretation of the Parasano fault scarp. The prominent white outcrops are the exposed fault plane along the fault scarp. (i) same view as (h) with no interpretation. (j) Outcrop view of the Parasano Scarp. Note the mass movement scars in the hangingwall, shown in more detail in (k) and located in (h). (k) view of the Mesozoic limestone fault plane exposed in a mass movement scar. View is in February, so the trees in the distance do not have leaves (compare with Google views). Black arrows show corrugations recording the movement direction on the fault. The half white arrow shows the downthrow of the Quaternary colluvium in the hangingwall. (l) Close up of the fault plane located in (k) showing frictional wear striae (white arrows) recording the movement direction across the fault. Finger for scale.

(g) Overview of the Parasano Scarp. (h) Interpretation of the Parasano fault scarp. The prominent white outcrops are the exposed fault plane along the fault scarp. (i) same view as (h) with no interpretation. (j) Outcrop view of the Parasano Scarp. Note the mass movement scars in the hangingwall, shown in more detail in (k) and located in (h). (k) view of the Mesozoic limestone fault plane exposed in a mass movement scar. View is in February, so the trees in the distance do not have leaves (compare with Google views). Black arrows show corrugations recording the movement direction on the fault. The half white arrow shows the downthrow of the Quaternary colluvium in the hangingwall. (l) Close up of the fault plane located in (k) showing frictional wear striae (white arrows) recording the movement direction across the fault. Finger for scale.

However, Roberts and Michetti (2004) and Papanikoloau and Roberts (2007) who mapped the geometry, kinematics and rates of deformation due to earthquakes since 12-18 ka show that spatial variation in fault slip occurs at a scale of tens of kilometres, whilst fault scarps have offsets of <30-40 metres and a geomorphic expression that can only be visualised on topographic images and photographs with spatial resolution at the metre-scale. The difference in scale between the observations and spatial variation, makes it difficult to visualise the deformation using conventional geological and topographic maps. As a result, there remains debate concerning the exact positions of active fault scarps (e.g. compare the fault maps of Valensise and Pantosti 2001, Roberts and Michetti 2004, Papanikoloau and Roberts 2007, Galadini and Galli 2000, Guidoboni et al. 2007, Ithaca Project 2007). This debate needs to be finalised because these earthquake-prone active faults are in an economically developed country with high population density, and the positions and dimensions of the active faults are necessary inputs into seismic hazard assessments (Pace et al. 2002, Roberts et al. 2004).

In this paper, Google Earth is used to map the positions and dimensions of active fault scarps at a regional scale (Figure 1b). The key features that allow recognition of active scarps in Google Earth that have previously been mapped in the field - that is, (1) SPOT images of the scarps themselves (Figure 2a) and (Figure 2b), (2) incised drainage in the uplifted footwalls of the scarps (Figure 3),

Figure 3. Examples of Incised Drainage

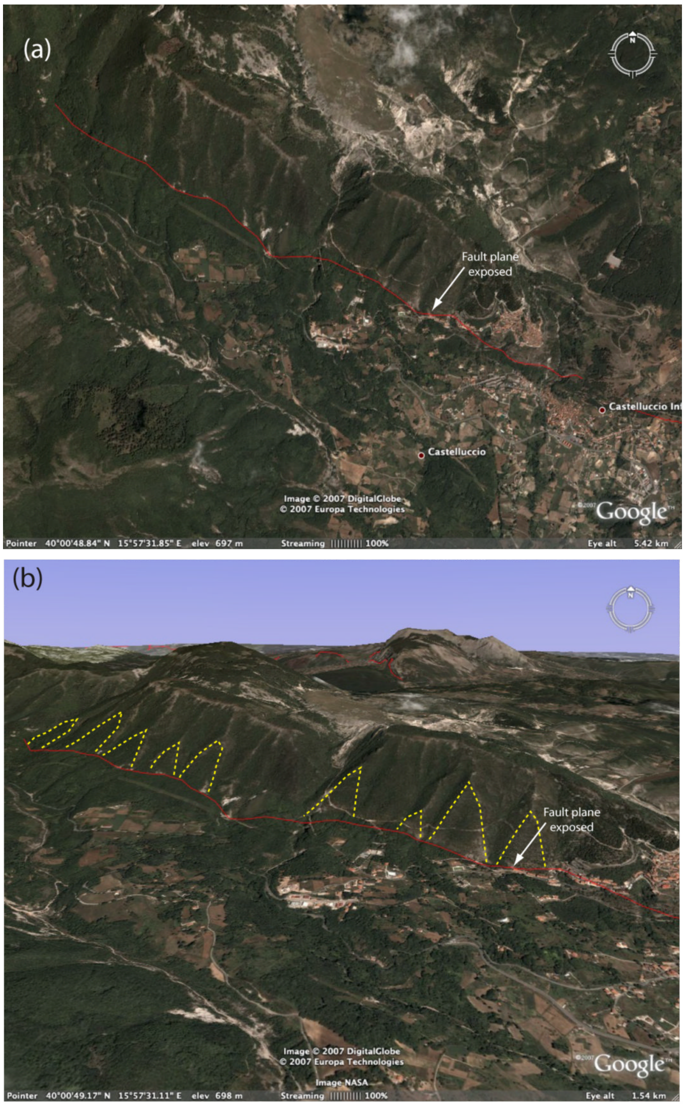

Figure 3. Examples of incised drainage in the uplifted footwalls of the scarps seen on Google Earth in map view (a) and 3D perspective (b). Note how the termination of incised drainage and triangular facets (interpreted in (b) with yellow dashed lines) define a lineament that defines the fault scarp. The fault plane is exposed behind a house where indicated.

Examples of incised drainage in the uplifted footwalls of the scarps seen on Google Earth in map view (a) and 3D perspective (b). Note how the termination of incised drainage and triangular facets (interpreted in (b) with yellow dashed lines) define a lineament that defines the fault scarp. The fault plane is exposed behind a house where indicated.

(3) oversteepened bases to escarpments in the footwall of the scarps (Figure 4) - can be visualised using the high photographic spatial resolution and the 3D rendition of the topography within Google Earth. The scarps can be digitised into Google Earth using a “path tool” (Figure 5). Extraction of precise latitudes and longitudes of paths that define the scarps could be used to assess the completeness and accuracy of existing maps of active faults

(Valensise and Pantosti 2001, Roberts and Michetti 2004, Papanikoloau and Roberts 2007, Galadini and Galli 2000, Guidoboni et al. 2007, Ithaca Project 2007).

Figure 4. Oversteepened escarpments

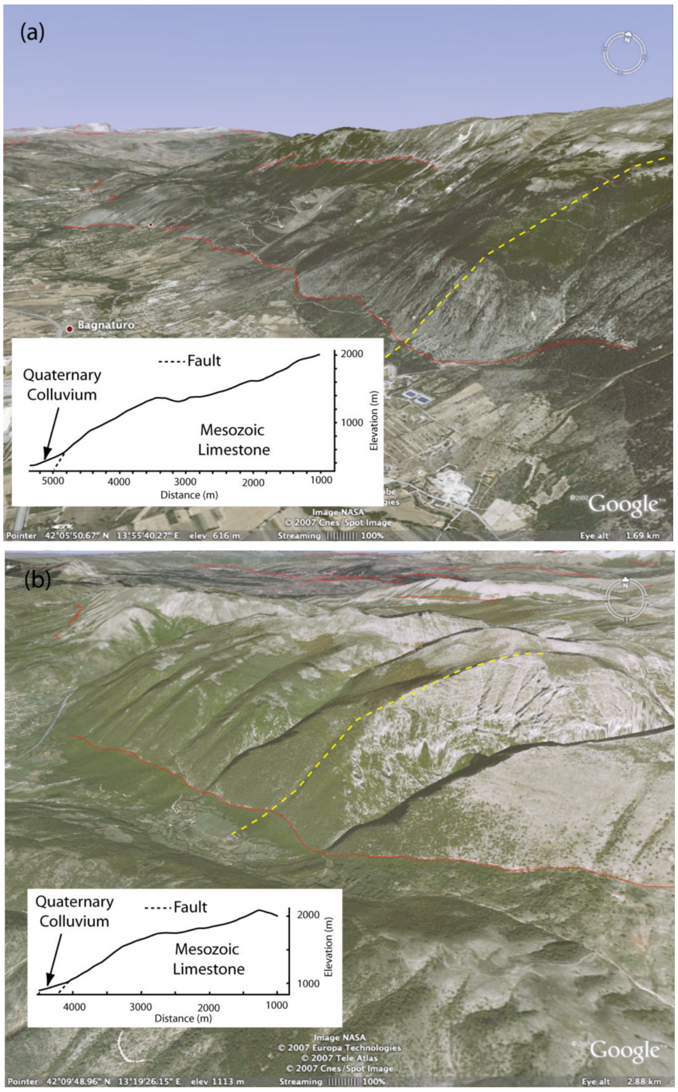

Figure 4 Oversteepened base fault escarpments. (a) Sulmona Fault. (b) Velino Fault. Topography from SRTM data. Dashed yellow lines locate the topographic profiles shown as insets. The topographic slopes within 1-2 km of the active niormal faults show steep slope relative to those further into the footwall. This is a characteristic feature of active normal faults where erosion rates are lower than fault slip rates and cannot maintain an equilibrium conave upwards hill slope.

Oversteepened base fault escarpments. (a) Sulmona Fault. (b) Velino Fault. Topography from SRTM data. Dashed yellow lines locate the topographic profiles shown as insets. The topographic slopes within 1-2 km of the active niormal faults show steep slope relative to those further into the footwall. This is a characteristic feature of active normal faults where erosion rates are lower than fault slip rates and cannot maintain an equilibrium conave upwards hill slope.

Figure 5. Parasano fault scarp

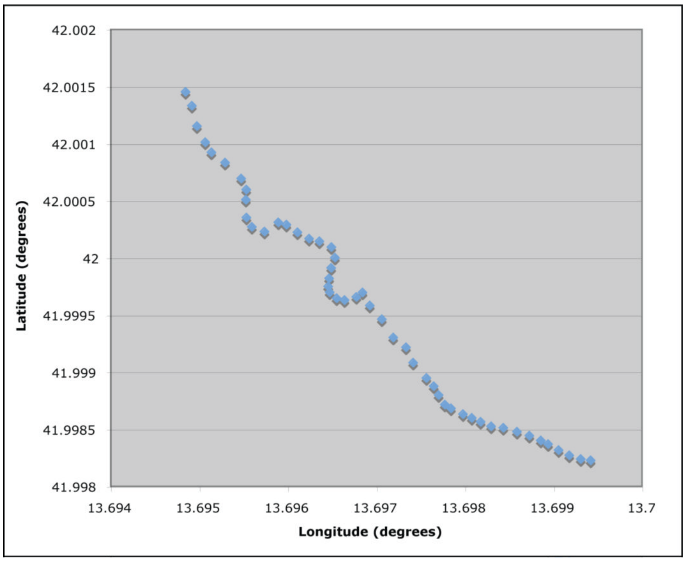

Figure 5. Precise geographic coordinates of the Parasano fault scarp extracted from a "path" drawn in Google Earth.

Precise geographic coordinates of the Parasano fault scarp extracted from a "path" drawn in Google Earth via a "kml file".

Method

The key features that allow recognition of active scarps are (1) detailed fieldwork where faults shown on existing geological maps are visited and assessed for fault activity (see Roberts and Michetti 2004, Papanikoloau and Roberts 2007 for details), (2) remotely-sensed (e.g. SPOT) images of the scarps themselves, (3) incised drainage in the uplifted footwalls of the scarps that are best-visualised in digital elevation models (DEMs), (4) escarpments in the footwall of the scarps, that show a variety of topographic features characteristic of active normal faulting such as triangular facets and oversteepened basal profiles (again, best-visualised in DEMs). This study details the results of fieldwork presented in Roberts and Michetti (2004) and Papanikoloau and Roberts (2007), that have now been correlated with observations from SPOT images and the DEM in Google Earth. This allows documentation of the precise latitudes and longitudes of paths that define the active fault scarps. First, images of typical landforms associated with scarps are presented, followed by a regional analysis of the fault scarps.

Results

The fieldwork revealed that fault scarps are clear in the landscape, and appear as limestone fault planes offsetting slopes that formed during the last glacial maximum (12-18 ka) (Fig. 2). The slopes are covered in tephra deposits derived from eruptions of volcanoes on the west coast of Italy (see Roberts and Michetti 2004 for a review of dates that confirm the last glacial maximum age of the landforms), and the fault planes themselves have been dated using ^{36}Cl exposure dating (Palumbo et al. 2006); dates confirm the scarps are 12-18 ka. These observations, together with palaeoseismological trench investigations (e.g. Pantosti et al. 1996, Michetti et al. 1996), and historical reports of earthquake surface ruptures (e.g. see Serva et al. 1986), reveal that earthquakes rupture the ground surface during events >Ms 5.5, with vertical surface displacements of c. 1 metre (depending on magnitude; Wells and Coppersmith 1994). Thus, scarps that are metres to tens of metres high record the cumulative effect of numerous palaeoearthquakes, and this is confirmed by ^{36}Cl exposure dating that has revealed 5-7 metre-scale surface exposure events on one fault that are interpreted as palaeoearthquakes (Palumbo et al. 2006).

The key observation in this paper is that such fault scarps can be seen clearly on SPOT images within Google Earth, and related to the larger-scale topography via observations of the DEM (Figure 3)and (Figure 4). The scarps appear as clear lines of limestone outcrop that occur where field observations confirm the existence of fault planes covered in striations and corrugations produced by frictional-slip during earthquakes (Roberts and Michetti 2004, Papanikolaou and Roberts 2007). The scarps commonly occur at the bases of oversteepened footwall escarpments (Figure 4), that in places show (1) triangular facets where spurs have been truncated by upward-propagating faults, and/or (2) incised drainage where fault slip has lowered the base-level of rivers, driving fluvial incision (Figure 3).

In places limestone outcrops along fault scarps visited during fieldwork are clear on the SPOT images and have clear oversteepened escarpments, triangular facets and incised drainage, but elsewhere scarps may not be obvious due to tree cover or lithologies that do not preserve surface displacements. Google Earth allows notes to be added facilitating documentation of the attributes that define interpretation of individual examples of scarps. Thus, some scarps are clearer than others, and this is indicated in the accompanying "kmz" file.

The exact positions of faults can be extracted from the “paths” defined in Google Earth, allowing precise x-y coordinate data to be made widely-available (e.g. Figure 5).

Mapping in this paper is limited to the area between the SE tip of the Pollino fault and the NW tip of the Rieti Fault. Other active faults are well-known to the NW and SE of this area but their traces are not shown here due to lack of fieldwork by the authors in these locations. Also, faults shown in red on Figure 1b have been visited in the field by the author, whilst those shown in white have not; the traces of faults shown in white, although constrained be geomorphic features visible in Google Earth, are therefore less certain than those shown in red.

The mapping reveals a regional pattern of active fault scarps that are sub-parallel to the length of the Italian Peninsula (Figure 1), but the faults are closer to the western coast in the south. Scarps are localised within the high mountains of the Apennines, and it is clear within Google Earth that no such scarps occur west or east of the reported examples, consistent with existing fault mapping (Valensise and Pantosti 2001, Roberts and Michetti 2004, Papanikoloau and Roberts 2007, Galadini and Galli 2000, Guidoboni et al. 2007, Ithaca Project 2007). In central Italy, up to 6-7 active normal faults faults exist on SW-NE traverses across the Apennines. There appear to be less faults in southern Italy, with a maximum of 2-3 faults on SW-NE traverses across the Apennines.

The traces of the faults appear discontinuous on Figure 1, with lines of scarps 20-40 km in length defined by shorter lines that are in places only a few kilometres in length. This does not reflect the actual displacement patterns on the faults, because Roberts and Michetti (2004) and Papanikolaou and Roberts (2007) show that total throws across the faults show offset profiles that decrease from maxima at fault centres to minima at lateral tips over distances of c. 20-40 km (Figure 6).

Figure 6. Regional fault map

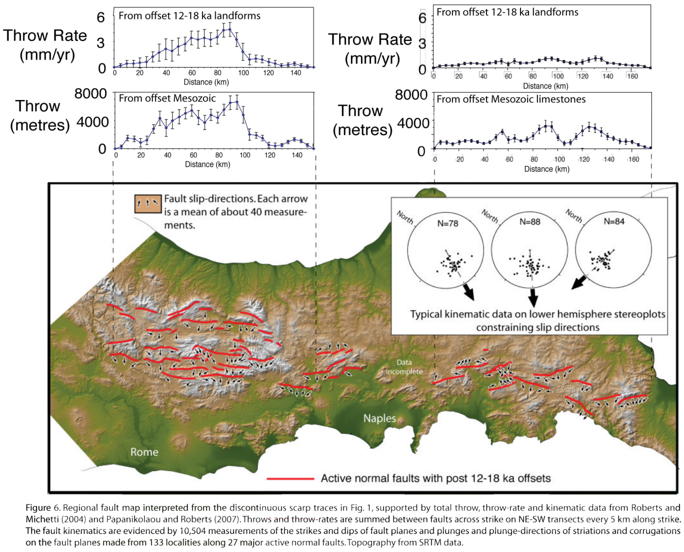

Regional fault map interpreted from the discontinuous scarp traces in Fig. 1, supported by total throw, throw-rate and kinematic data from Roberts and Michetti (2004) and Papanikolaou and Roberts (2007). Throws and throw-rates are summed between faults across strike on NE-SW transects every 5 km along strike. The fault kinematics are evidenced by 10,504 measurements of the strikes and dips of fault planes and plunges and plunge-directions of striations and corrugations on the fault planes made from 133 localities along 27 major active normal faults. Topography from SRTM data.

Consistency between along-strike stretching of the ground surface due to these throw variations and fault kinematics is recorded by 10,504 measurements of the strikes and dips of fault planes and plunges and plunge-directions of striations and corrugations on the fault planes made from 133 along 27 major active normal faults (summarised in Figure 6). Convergent patterns of fault-slip on individual faults occurs on the same length scale as throw variations indicating that structural segmentation of the fault system occurs at the 20-40 km lengths scale. These interpreted faults, along with their throw patterns, throw-rate patterns and kinematics are summarised on Figure 6. The discontinuities on the scale of a few kilometres do reflect the discontinuous visualisation of the scarps allowed by forest cover (where trees can be higher than scarps and hence obscure their traces on SPOT images), and lack of scarp preservation where the bedrock shows a high propensity to erosion and mass transport. Thus, comparison of Figure 1 and Figure 6 allow visualisation of the positions of faults scarps that are clear in the geomorphology along longer faults.

Segmentation defined in this way, with 20-40 km faults, reveals that the fault system is composed predominantly of soft-linked faults arranged in both en echelon and end-on geometries. Faults are separated by relay-ramps that in places contain dip-slip release faults allowing extension along strike due to throw-gradients on the main NW-SE faults. However, no examples of strike-slip transfer faults linking displacements on one NW-SE fault are, in the opinion of the author, clear in the geomorphology. This lack of transverse strike-slip lineaments is real because in many instances, the ground in these relay zones is extremely well-exposed, and it is not feasible that scarps would not be seen on the available SPOT images. Segmentation at this crustal scale is characterised by along-strike fault overlaps across relay zones of less than a few tens of percent of fault lengths and across strike distances across relay zones of 5-15 km.

Discussion

Debate is ongoing concerning the numbers, geometries and actual positions of active normal faults in the Italian Apennines (compare the fault maps of Valensise and Pantosti 2001, Roberts and Michetti 2004, Papanikolaou and Roberts 2007, Galadini and Galli 2000, Guidoboni et al. 2007, Ithaca Project 2007). This, in the view of the authors, has in part been due to the difficulty in visualising regional patterns of deformation from observations of geomorphic features that need to be viewed at a metre-scale spatial resolution; Google Earth now allows such visualisation and quantification of the active fault geometries (Figure 1) and (Figure 6). It is the opinion of the author that such visualisation is the way to conclude such debates with agreement needed in the near future on a final active fault map. However, it is clear from the relatively discontinuous nature of the scarps seen with Google Earth, and the relatively continuous throw and kinematic variations along the faults (Figure 6) that one cannot simply use Google Earth to map such faults without detailed fieldwork. In particular, the kinematic data are extremely useful in helping define fault lengths, and such data can only be collected at outcrop at present (Roberts 1996, 2006, Roberts and Michetti 2004, Papanikolaou and Roberts 2007).

It is important to correctly identify the numbers, geometries and actual positions of active normal faults in the Italian Apennines and elsewhere, because these are the seismogenic sources that certainly control the locations of future devastating earthquakes, and possibly the maximum magnitudes of expected earthquakes (Wells and Coppersmith 1994, Pace et al. 2002). Through comparison of multi-seismic-cycle strain-rates defined by slip across fault scarps and single-seismic-cycle strain rates from instrumental seismicity and geodesy (e.g. Roberts 2006), one may be able to constrain the stress-loading and strain-release patterns that govern earthquake recurrence, through improved understanding of the mechanics of the seismic cycle; visualisation of active fault geometries is a key waypoint on the journey to this goal.

Conclusions

Google Earth has been used to map active normal fault scarps that offset 12-18 ka landforms in the Apennines, Italy. This map provides precise locations for structures responsible for tectonic strain release and earthquake rupture. Spatial variation in fault slip occurs at a scale of tens of kilometres, whilst fault scarps have offsets of <30-40 metres and a geomorphic expression that can only be visualised on topographic images with spatial resolution at the metre-scale. Thus, until now, debate has surrounded the exact positions of scarps due, in part, to problems of visualising both the detailed geomorphic features and their regional variation. Provision of complete SPOT image coverage and topography within Google Earth allows individual scarps visited during fieldwork to be visualised at a regional scale within an easily-accessible interface. The resultant fault map is an important step towards agreement on a final fault map, which is needed to facilitate comparison of multi-seismic-cycle strain-rates defined by slip across fault scarps and single-seismic-cycle strain rates from instrumental seismicity and geodesy. Such a comparison is needed to constrain the stress-loading and strain-release patterns that govern earthquake recurrence, through improved understanding of the mechanics of the seismic cycle.

Acknowledgements

The work was funded by NERC Grants NE/E01545X/1, NE/B504165/1, and GR9/02995, and Birkbeck, University of London. Discussions with Alessandro Michetti, Patience Cowie, Ioannis Papanikolaou, Nigel Morewood, Joanna Faure Walker, Eutizio Vittori, Alex Whittaker, Mikael Attal and Greg Tucker are gratefully acknowledged.

References

Anderson, H., Jackson, J.,1987. Active tectonics of the Adriatic region. Geophysical Journal of the Royal Astronomical Society, 91, 937-983.

Galadini, F., Galli, P., 2000. Active tectonics in the central Apennines (Italy) – Input data for seismic hazard assessment. Natural Hazards, 22, 225-270. 10.1023/A:1008149531980

Giraudi, C., 1995. I detriti di versante al margin della piana del Fucino (Italia centrale): significato palaeoclimatico ed impatto antropico. Il Quaternario, 8, 203-210.

Guidoboni E., G. Ferrari, D.Mariotti, A.Comastri, G.Tarabusi and G.Valensise 2007 - CFTI4Med, Catalogue of Strong Earthquakes in Italy (461 B.C.-1997) and Mediterranean Area (760 B.C.-1500). INGV-SGA. Available from http://storing.ingv.it/cfti4med/.

Ithaca Project 2007. http://www.apat.gov.it/site/en-GB/Projects/ITHACA_-_ITaly_HAzards_from_CApable_faults/

Margottini, C., Screpanti, A., 1988. Temporal evolution of the seismic crisis related to the 13th January 1915, Avezzano earthquake, in "Historical seismicity of central-eastern mediterranean region", Proceedings of the 1987 ENEA-IAEA International Workshop, edited by Margottini C. and L. Serva, 185-193, ENEA, Roma.

Michetti, A. M., Brunamonte, F., Serva, L., Vittori, E., 1996. Trench investigations of the 1915 Fucino earthquake fault scarps (Abruzzo, Central Italy): geological evidence of large historical events. Journal of Geophysical Research, 101, 5921-5936. 10.1029/95JB02852

Pace, B., Peruzza, L., Lavecchia, G., Boncio, P., 2002. Seismogenic sources in central Italy: from causes to effects. Mem. Soc. Geol. It., 57, 419-429.

Palumbo, L., L. Benedetti, D. Bourles, A. Cinque, R. Finkel, 2004. Slip history of the Magnola fault (Apennines, Central Italy) from 36Cl surface exposure dating: evidence for strong earthquakes over the Holocene, Earth Planet. Sci. Lett. 225, 163-176. 10.1016/j.epsl.2004.06.012

Pantosti, D., D'Addezio, G., Cinti, F., 1996. Paleoseismicity of the Ovindoli-Pezza fault, central Apennines, Italy: a history including a large, previously unrecorded earthquake in the Middle Ages (860-1300 A.D.). Journal of Geophysical Research. 101, 5937-5960. 10.1029/95JB03213

Papanikoloau, I., Roberts, G. P., 2007. Geometry, kinematics and deformation rates along the active normal fault system in the southern Apennines: implications for fault growth. Journal of Structural Geology, 29, 166-188. 10.1016/j.jsg.2006.07.009

Roberts, G. P., 1996. Variation in fault-slip directions along active and segmented normal fault systems, Journal of Structural Geology, 18, 835-845. 10.1016/S0191-8141(96)80016-2

Roberts, G. P., 2006. Multi-seismic cycle velocity and strain fields for an active normal fault system, central Italy. Earth and Planetary Science Letters, 252, 44-51. 10.1016/j.epsl.2005.11.066

Roberts, G. P., Michetti, A. M., 2004. Spatial and temporal variations in growth rates along active normal fault Systems: an example from Lazio-Abruzzo, central Italy. Journal of Structural Geology, 26, 339-376. 10.1016/S0191-8141(03)00103-2

Roberts, G. P., P. Cowie, I. Papanikoloau, Michetti. A. M., 2004. Fault scaling relationships, deformation rates and seismic hazards: an example from Lazio-Abruzzo region, central Italy. Journal of Structural Geology, 26, 377-398. 10.1016/S0191-8141(03)00104-4

Serva, L., Blumetti, A. M., Michetti, A. M. 1986. Gli effetti sul terreno del terremoto del Fucino (13 Gennaio 1915); tentative di interpretazione della evoluzione tettonica recente di alcune strutture. Mem. Soc. Geol. It., 35, 893-907.

Valensise, G., Pantosti, D., 2001. The investigation of potential earthquake sources in peninsular Italy: A review. Journal of Seismology, 5, 287-306. 10.1023/A:1011463223440

Wells, D. I., Coppersmith, K. J., 1994. New empirical relationships among magnitude, rupture length, rupture width, rupture area, and surface displacement. Bulletin of the Seismological Society of America, 84, 974-1002.